Nickel (II) Mediated In-situ Complex Formation with unexpected Ligand Transformations: Crystal Structures, DFT calculations and Catalytic Activity in CO_2 Fixation Reaction

Malay Dolai[a,], Urmila Saha[b], Juli Nanda Goswami,[a] Biswajit Bhattacharya[c], Franziska Emmerling[c] Ahmad A. Ifseisi,[d] and Surajit Biswas[e,*]*

a. *Department of Chemistry, Prabhat Kumar College(Vidyasagar University), Purba Medinipur 721404, W.B., India; E-mail-dolaimalay@yahoo.in*
b. *Department of Chemistry, Indian Association for the Cultivation of Science, Raja SC Mullick Road, Kolkata 700032, W.B., India.*
c. *BAM Federal Institute for Materials Research and Testing, Richard-Willstätter-Str. 11 12489 Berlin, Germany.*
d. *Department of Chemistry, University of Kalyani, Kalyani, Nadia, 741235, W.B., India.*
e. *Department of Chemistry, College of Science, King Saud University, Riyadh, 11451, Saudi Arabia.*

Experimental Section

Materials and Methods

The starting materials such as 2-cyano pyridine and 2-cyano pyrimidine, hydroxylamine hydrochloride (Sigma Aldrich) were used for the preparation of ligand. $NiCl_2.6H_2O$ (Merck, Germany) was used to prepare complex. Solvents like ethanol and methanol (Merck, India) were of reagent grade and dried before use. All other solvents and chemicals were of reagent grade, obtained from commercial sources and used without further purification.

Physical measurements

Elemental analyses were carried out using a Perkin–Elmer 240 elemental analyzer. Infrared spectra (400–4000 cm^{-1}) were recorded from KBr pellets on Perkin Elmer FTIR spectrometers. ^{1}H-NMR was recorded in DMSO-d_6 on a Bruker 300MHz NMR spectrometer using tetramethylsilane ($\delta = 0$) as an internal standard.

The carbonates products were identified over a Varian 3400 gas chromatograph (GC) fitted to a 30 m CP-SIL 8CB capillary column with a facility of flame ionization detector and hydrogen as the carrier gas. The

conditions used were: initial temperature 50°C, hold at initial temperature for 3 minutes then ramp rate 25°C/min to 350°C; hold at final temperature for 4 minutes. After completion of each catalytic reaction 10 mL ethyl acetate was added to the reaction mixture for quenching the reaction. Then the solution was washed with distilled H_2O (10 ml) five times. The collected organic part was dried over Na_2SO_4 (anhydrous) and evaporated to dryness on a rotary evaporator. Then obtained crude product finally was injected to Gas Chromatography to check conversion and identification of the product.

All substrate gave us only one sole product, no by-products are obtained from any substrate. So only one peak is obtained (except solvent peak) for those substrates whose conversion is 100% and two peaks (one for substrate and other for product, except solvent peak) obtained when substrate conversion is not 100%. In each case GC yield is determined using 'Area Percent Method'. Peak position of various reaction products was compared and matched with the retention times of authentic samples.

Single Crystal X-ray Crystallography

Single crystal X-ray diffraction of the complexes **1** and **2** were collected at low temperature (150 K) with monochromated Mo-Kα radiation (λ = 0.71073 Å) on a Bruker Kappa APEX II diffractometer equipped with a CCD area detector. Data reduction was carried out using the SAINT-Plus software package.[1] Multi-scan absorption correction was applied to all intensity data using the SADABS program.[2] The structure was refined via full matrix least squares on F^2 using the SHELX-2014 suite.[3] All non-hydrogen atoms were refined with anisotropic thermal parameters. The C-H hydrogen atoms were included in the structure factor calculations in geometrically idealized positions with isotropic thermal displacements depending on the parent atom, using a riding model.[4] Molecular diagrams[5] were drawn with Mercury 3.0. The crystal data and selected refinement details are listed in Table S1. The structures were deposited with the Cambridge Crystallographic Data Centre with the number 2345589-2345590.

Table S1. Crystal data and details of refinement for complexes **1** and **2**.

	1	**2**
Formula	$C_{24}H_{20}N_{10}Ni$	$C_{33}H_{44}Cl_4N_{18}Ni_2O_{11}$
Formula Weight	507.21	1136.20
Crystal System	Monoclinic	Monoclinic
Space group	*P21/n (No. 14)*	*C2/c (No. 15)*
a /Å *b* /Å *c* /Å	6.129(2) 15.814(6) 11.441(4)	21.354(3) 10.5144(13) 21.722(3)
α /°	90	90

β /° γ /°	102.800(14) 90	103.013(5) 90
V /Å^3	1081.4(7)	4751.7(10)
Z	2	4
D(calc) /g/cm^3	1.558	1.588
μ(MoK$_\alpha$) /mm	0.935	1.092
F(000)	524	2342
Theta min-max /°	2.2 - 27.6	2.2 - 26.8
hkl min/max	-7: 7 ; -20: 20 ; -14: 14	-26: 26 ; -13: 13 ; -27: 27
Reflections collected	21742	30906
Unique data, R(int)	2478, 0.060	5065, 0.0510
Observed data [*I*> 2σ(*I*)]	2098	4183
Parameters refined	169	347
GOF *R*1, w*R*2 [*I*> 2σ(*I*)] Residuals e. Å^{-3}	1.07 0.0295, 0.0695 -0.42, 0.41	1.06 0.0408, 0.1121 -0.62, 0.79

Table S2. Selected bond distances (Å) and angles (°) of complexes **1-2.**

Complex -1		**Complex -2**	
Ni1-N1	1.9347(18)	Ni1-Cl1	2.3869(7)
Ni1-N2	1.9424(18)	Ni1-O2	2.1240(17)
Ni1-N1a	1.9347(18)	Ni1-N1	2.096(2)
Ni1-N2a	1.9424(18)	Ni1-N2	2.019(2)
		Ni1-N3	2.087(2)
		Ni1-N8	2.094(2)
N1 -Ni1 -N2	86.99(7)	Cl1 -Ni1 -O2	169.63(18)
N1-Ni1-N1a	180.00	Cl1 -Ni1 -N1	101.2(2)
N1-Ni1-N2a	93.01(7)	Cl1 -Ni1 -N2	97.9(2)
N1a -Ni1-N2	93.01(7)	Cl1 -Ni1 -N3	90.3(2)
N2-Ni1-N2a	180.00	Cl1 -Ni1 -N8	91.6(2)
N1a -Ni1-N2a	86.99(7)	O2 -Ni1 -N1	84.6(3)
		O2 -Ni1 -N2	91.6(3)
		O2 -Ni1 -N3	87.7(3)
		O2 -Ni1-N8	78.8(3)
		N1-Ni1-N2	78.2(3)
		N1-Ni1-N3	155.5(3)

		N1-Ni1-N8	100.7(4)
		N2 -Ni1-N3	78.8(3)
		N2-Ni1-N8	170.4(3)
		N3-Ni1-N8	100.5(3)
		Cl1-Ni2 -O2a	168.23(18)

Table S3. Hydrogen bond parameters for complex **1** (Å /°).

D-H…A	d(D-H)	d(H..A)	<DHA	d(D..A)	Symmetry code
N1-H1…N5	0.91(2)	2.22(2)	114.5(18)	2.726(2)	intramolecular
N2-H2...N4	0.92(2)	2.21(2)	114.5(18)	2.721(3)	intramolecular

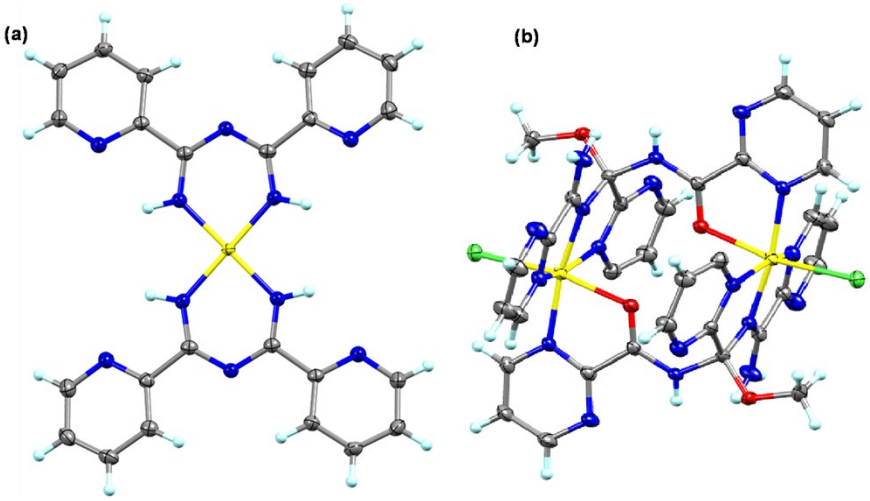

Figure S1. Thermal ellipsoid drawing of the asymmetric unit of complexes **1** and **2** with 50% ellipsoids probability.

Computational details

To study and understand the mechanistic pathway of the current ligand transformation study from the molecular level, the density functional theory (DFT)[6] computations were performed through GAUSSIAN 09. The individual roles of the steps and support have been studied. All the ground state electronic structure calculations in gas phase for all steps involved in the ligand transformations have been carried out using DFT[6] method and Becke's hybrid function[7] with the Lee-Yang-Parr (LYP) correlation function[8] was used for the study to justify the proper geometries and electronic properties.

For H atoms we used 6-31(g) basis set; for C, N, O atoms we employed 6-31G as basis set for all the calculations. All the calculations were performed with the Gaussian 09W software package.[9]

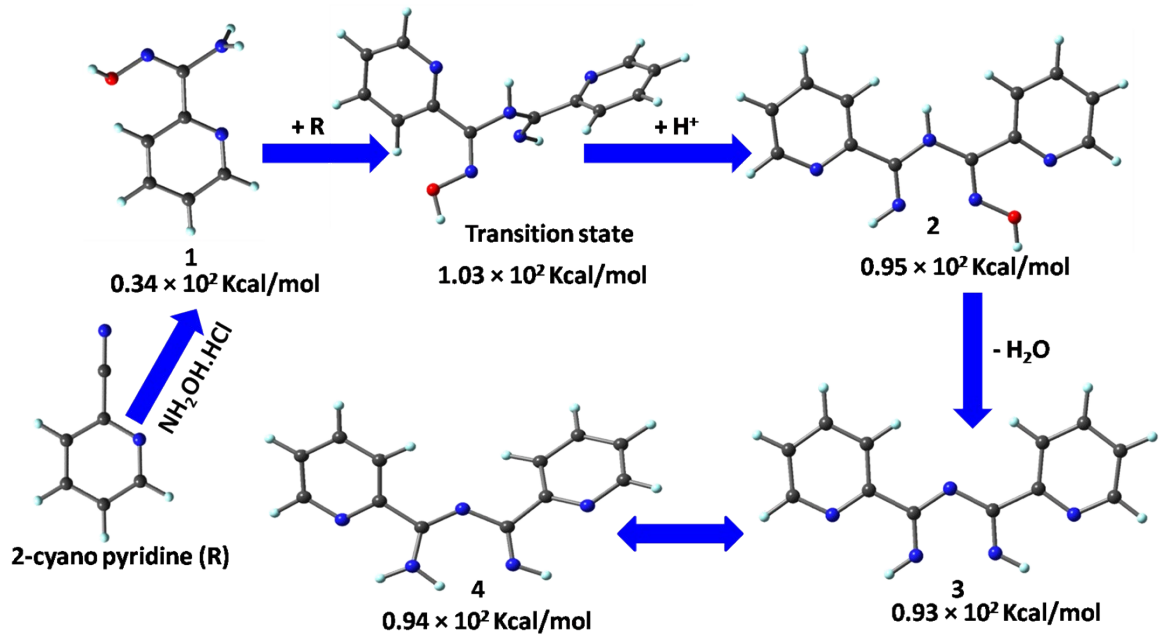

Fig. S2. DFT optimized structures with their relative energies for ligand transformation in complex **1**.

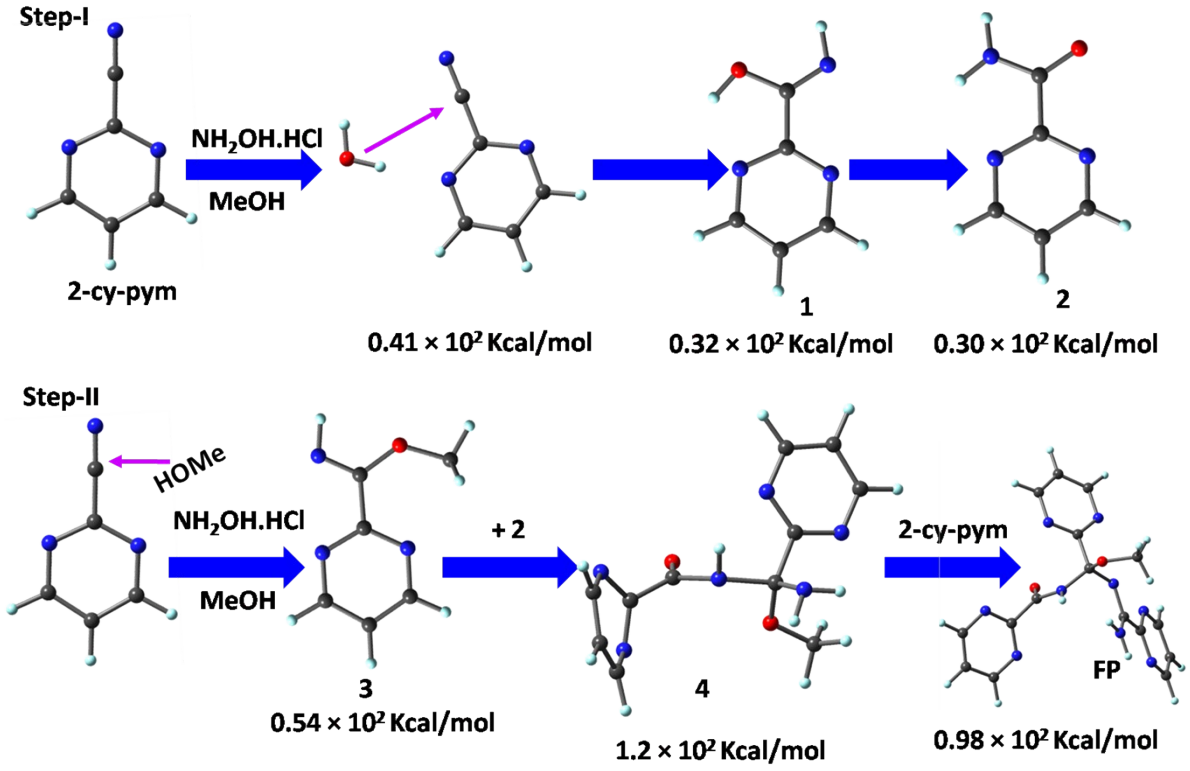

Fig. S3. DFT optimized structures with their relative energies for ligand transformation in complex **2**.

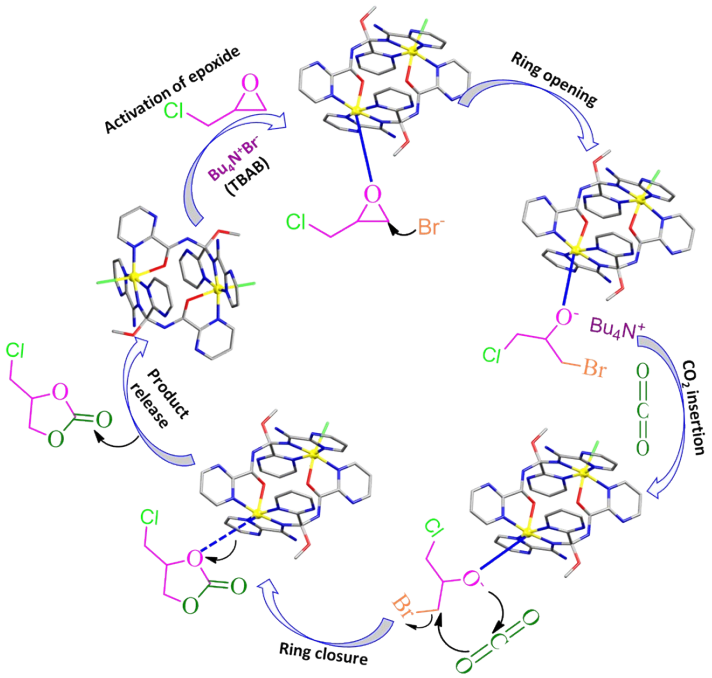

Fig. S4. Probable mechanistic pathway for the catalytic cycloaddition of CO_2 with epoxides in presence of complex **2**.

General procedure of catalytic synthesis of organic cyclic carbonates by the cyclo-addition of carbon dioxide to epoxides

Epoxides (15 mmol) and catalyst (0.05 mol%) were mixed together in a 20 ml round bottomed flask followed by the addition of tetrabutyl ammonium bromide (TBAB) (0.2 mol%). The mixture was stirred at 60ºC and 1 bar pressure of CO_2 using balloon set up. The progress of the reaction was monitored through thin layer chromatography. 10 mL ethyl acetate was added to the reaction mixture after quenching the reaction. Then the solution was washed with distilled H_2O (10 ml) five times. The collected organic part was dried over Na_2SO_4 (anhydrous) and evaporated to dryness on a rotary evaporator. Finally, the mixture was injected to Gas Chromatography to check conversion and identification of the product. The pure cyclic carbonates products were separated through silica gel column chromatography using hexane and ethyl acetate mixture as eluent. ^1H NMR spectroscopy was done for further characterization of the obtained product.

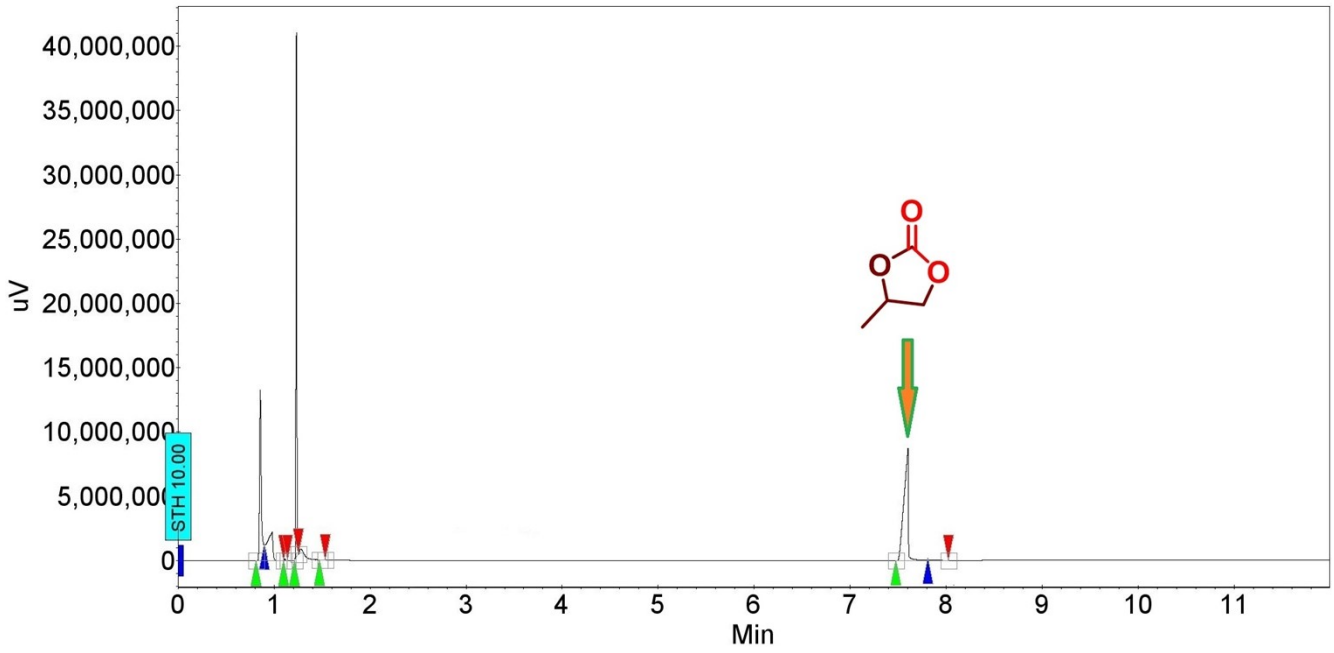

Figure S5: GC chromatogram for the catalytic synthesis of 4-methyl-1,3-dioxolan-2-one.

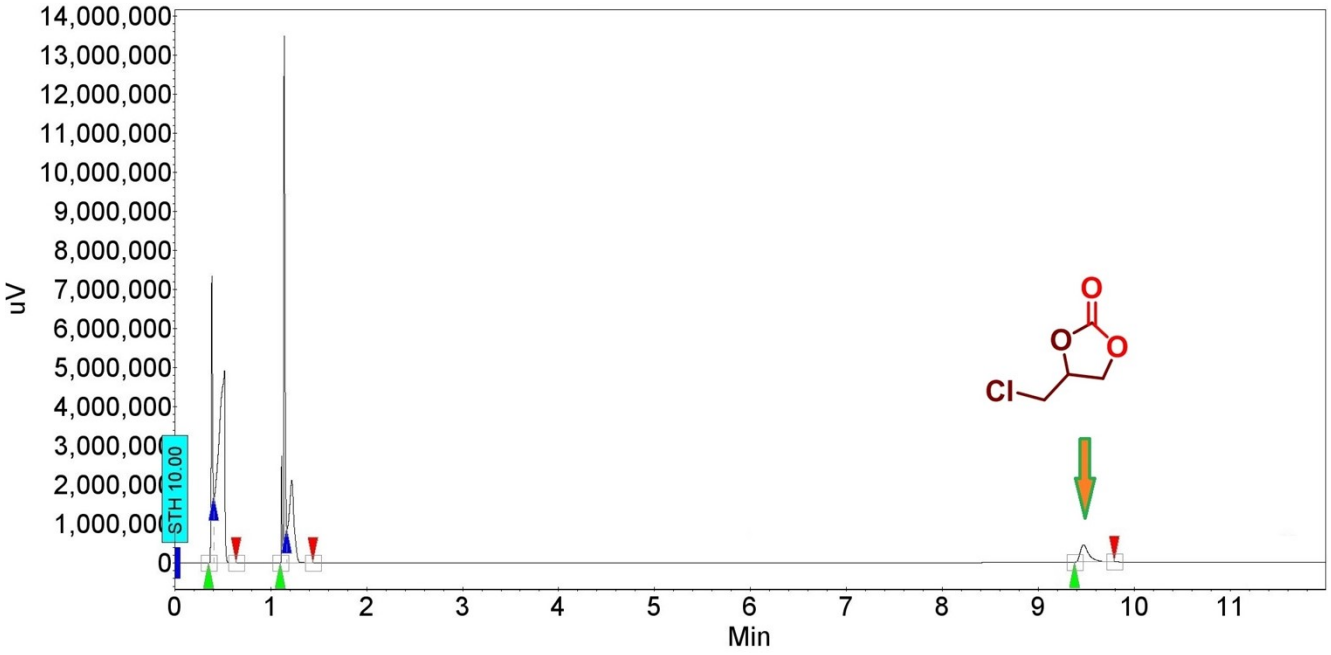

Figure S6: GC chromatogram for the catalytic synthesis of of 4-(chloromethyl)-1,3-dioxolan-2-one.

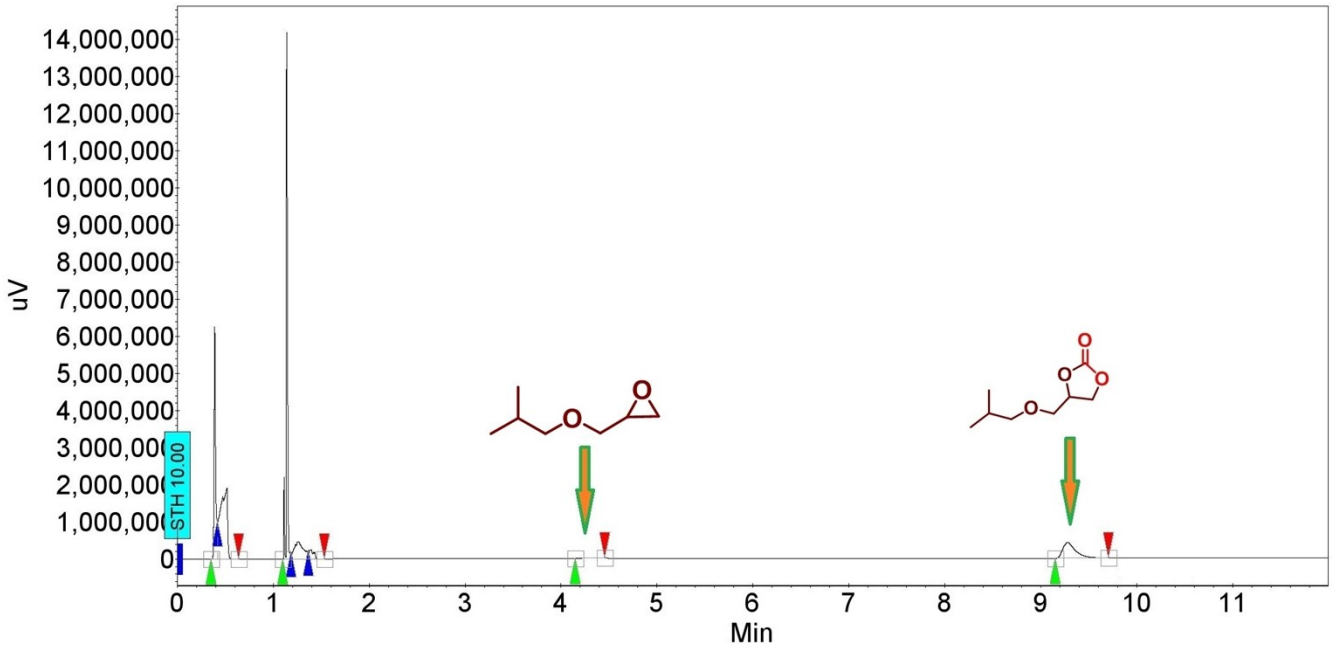

Figure S7: GC chromatogram for the catalytic synthesis of 4-isobutoxy-1,3-dioxolan-2-one.

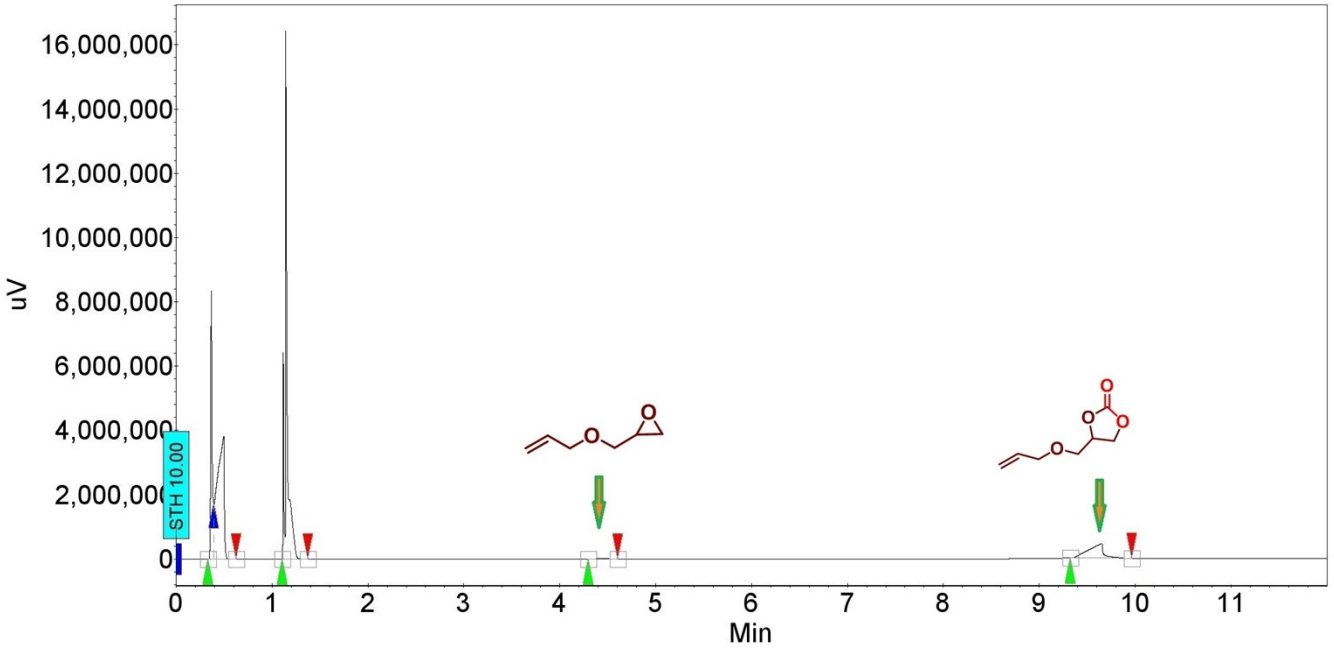

Figure S8: GC chromatogram for the catalytic synthesis of 4-((allyloxy)methyl)-1,3-dioxolan-2-one.

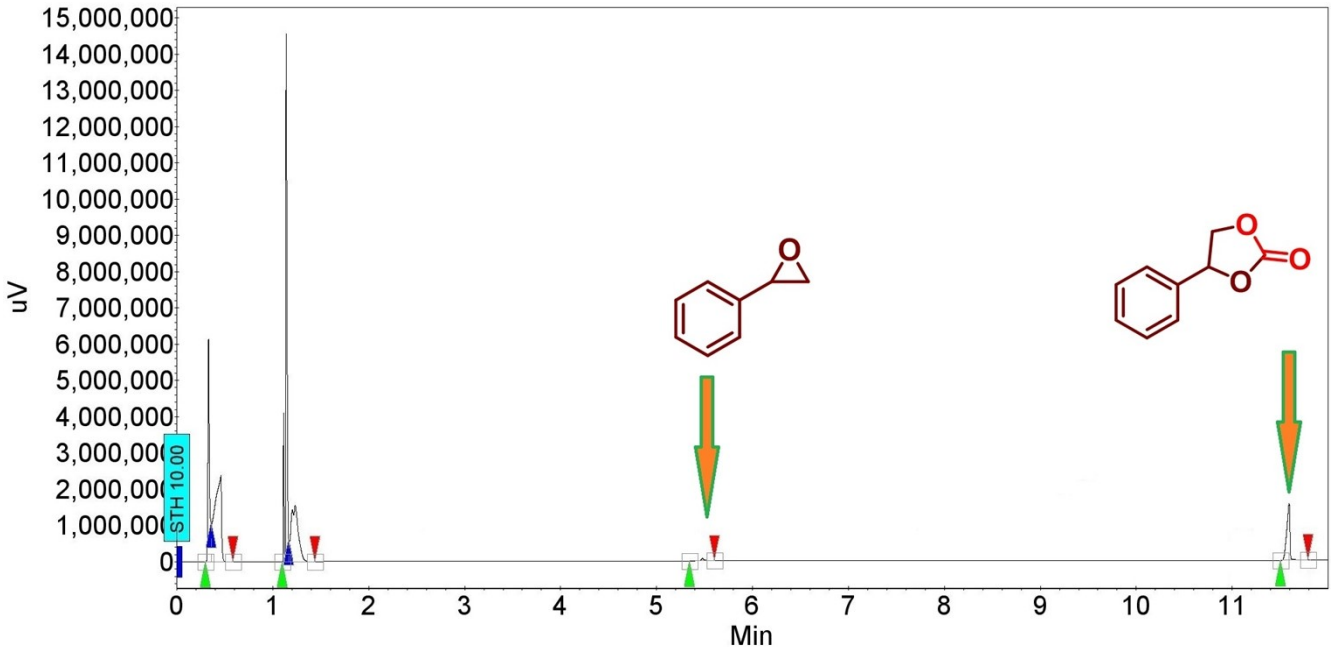

Figure S9: GC chromatogram for the catalytic synthesis of 4-phenyl-1,3-dioxolan-2-one.

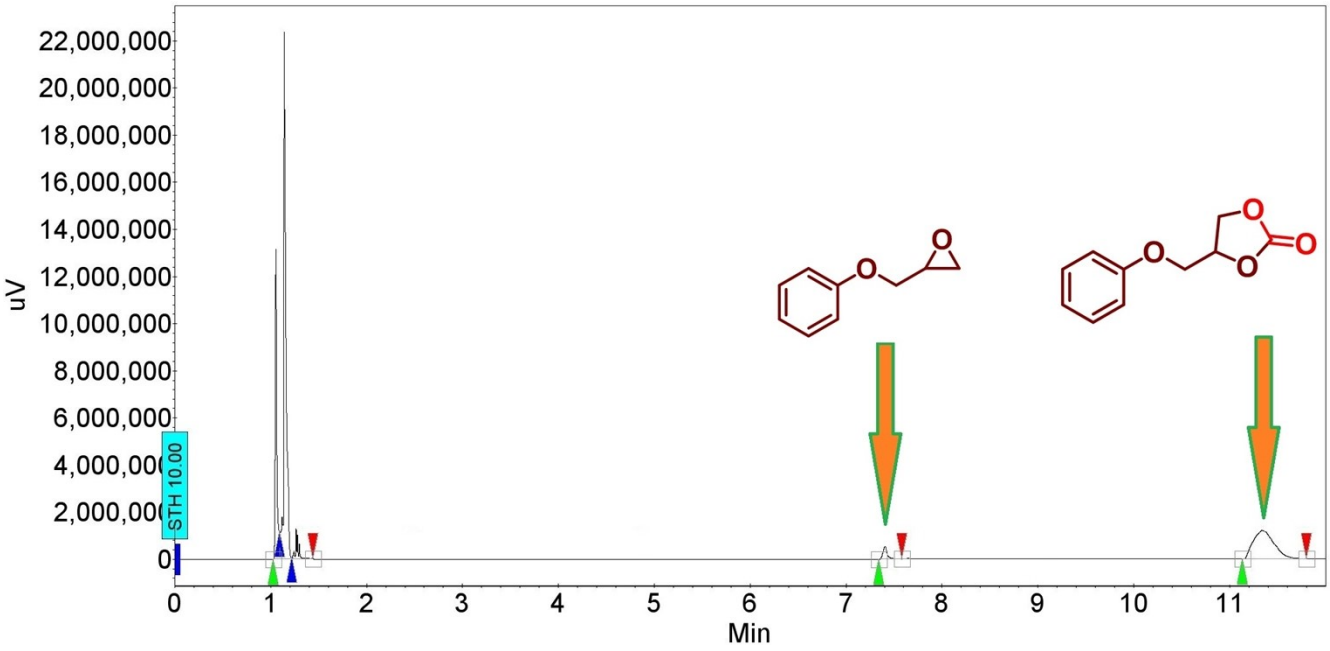

Figure S10: GC chromatogram for the catalytic synthesis of 4-(phenoxymethyl)-1,3-dioxolan-2-one.

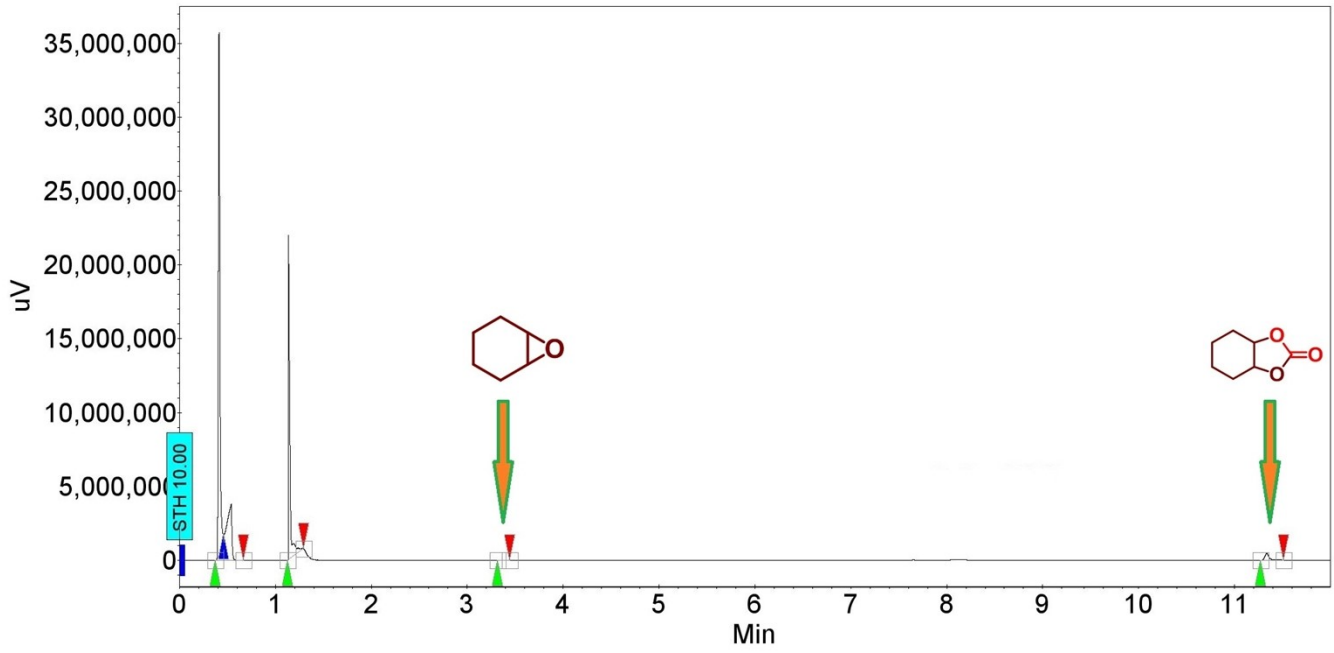

Figure S11: GC chromatogram for the catalytic synthesis of hexahydrobenzo[d][1,3]dioxol-2-one.

^{1}H NMR data of cyclic carbonates.[10]

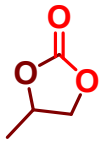	Yellowish oil, **^{1}H NMR (400 MHz, $CDCl_3$)** δ 1.252 (d, *J* = 4.0 Hz, 3H), 3.923 (t, *J* = 6.8 Hz, 1H), 4.217 (t, *J* = 7.2 Hz, 1H), 4.809-4.869 (m, 1H) ppm.
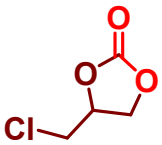	Yellowish oil, **^{1}H NMR (400 MHz, $CDCl_3$)** δ 3.610-3.704 (m, 2H), 4.648 (t, *J* = 6.8 Hz, 1H), 4.725-4.772 (m, 1H), 4.868-5.004 (m, 1H) ppm.
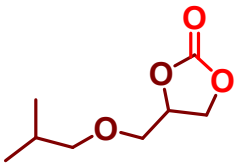	Yellowish oil, **^{1}H NMR (400 MHz, $CDCl_3$)** δ 1.145 (d, *J* = 3.6 Hz, 6H), 3.581-3.697 (m, 3H), 4.331-4,373 (m, 1H), 4.483 (t, *J* = 7.6 Hz, 1H), 4.773-4.853 (m, 1H) ppm.
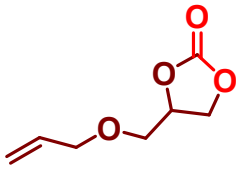	Colourless liquid; **^{1}H NMR (400 MHz, $CDCl_3$)** δ 3.356-3.553 (m, 2H), 3.942-4.033 (m, 2H), 4.282-4.356 (m, 1H), 4.395-4.474 (m, 1H), 4.702-4.807 (m, 1H), 5.077-5.243 (m, 2H), 5.653-5.751 (m, 1H) ppm.

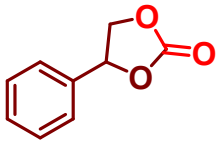	White solid, **^{1}H NMR (400 MHz, $CDCl_3$)**: δ 4.198 (t, *J* = 7.6 Hz, 1H), 4.454 (d, *J* = 7.6 Hz, 1H), 4.907-4-942 (m, 1H), 7.358 (t, *J* = 7.6 Hz, 2H), 7.442-7.484 (m, 3H) ppm.
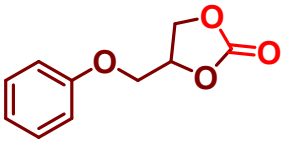	Yellowish oil, **^{1}H NMR (400 MHz, $CDCl_3$)** δ 4.066-4.101(m, 1H), 4.173-4.212 (m, 1H), 4.477-4.505 (m, 1H), 4.534-4.588 (m, 1H), 4.925-4.976 (m, 1H), 6.854-6.893 (m, 2H), 6.939-7.003 (m, 1H), 7.232-7.292 (m, 2H) ppm.
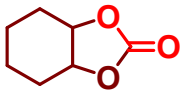	Colourless liquid, **^{1}H NMR (400 MHz, $CDCl_3$)**: δ 1.356-1.499 (m, 2H), 1.585-1.676 (m, 2H), 2.178 (t, *J* = 4.4 Hz, 4H), 4.621-4.787 (m, 2H) ppm.

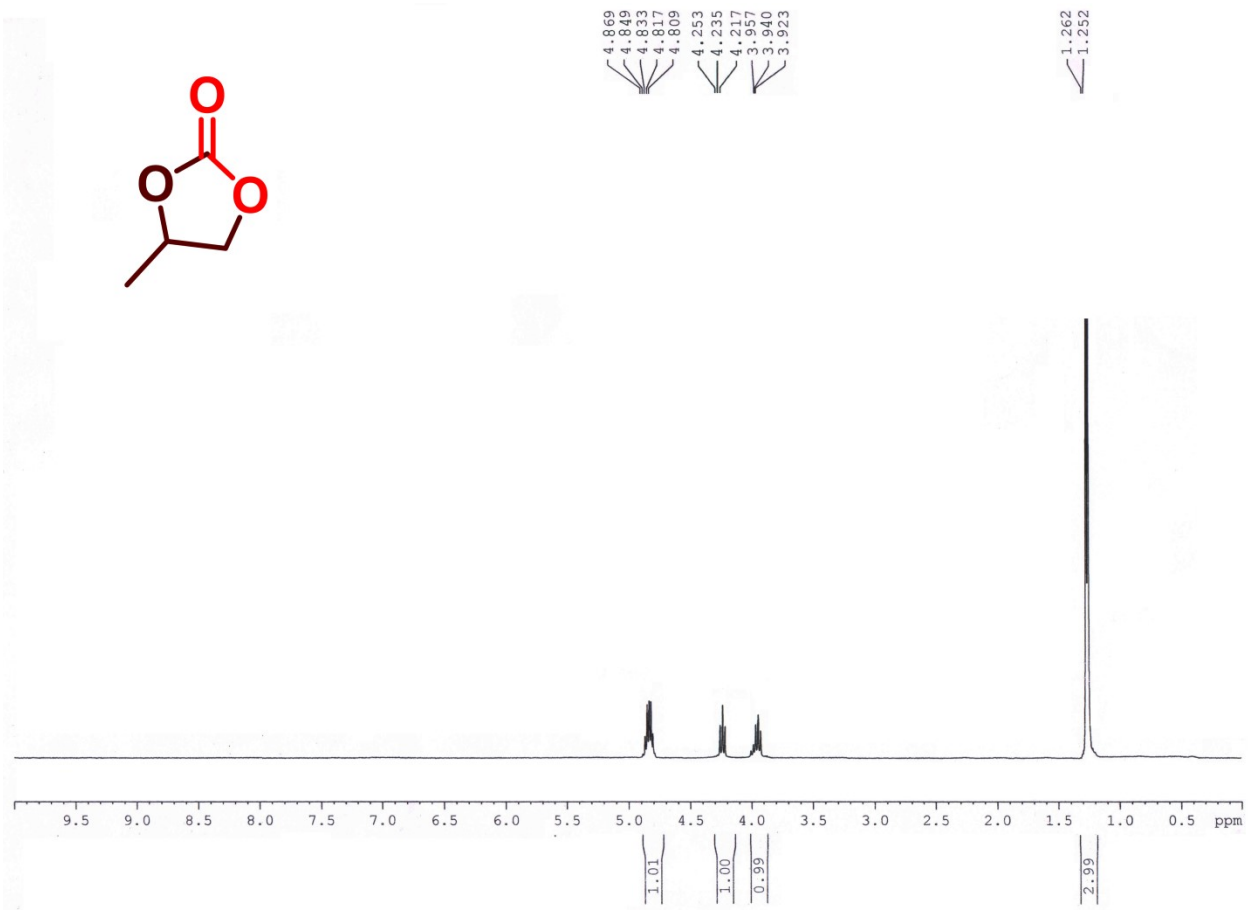

Figure S12: ^{1}H NMR spectra of 4-methyl-1,3-dioxolan-2-one.

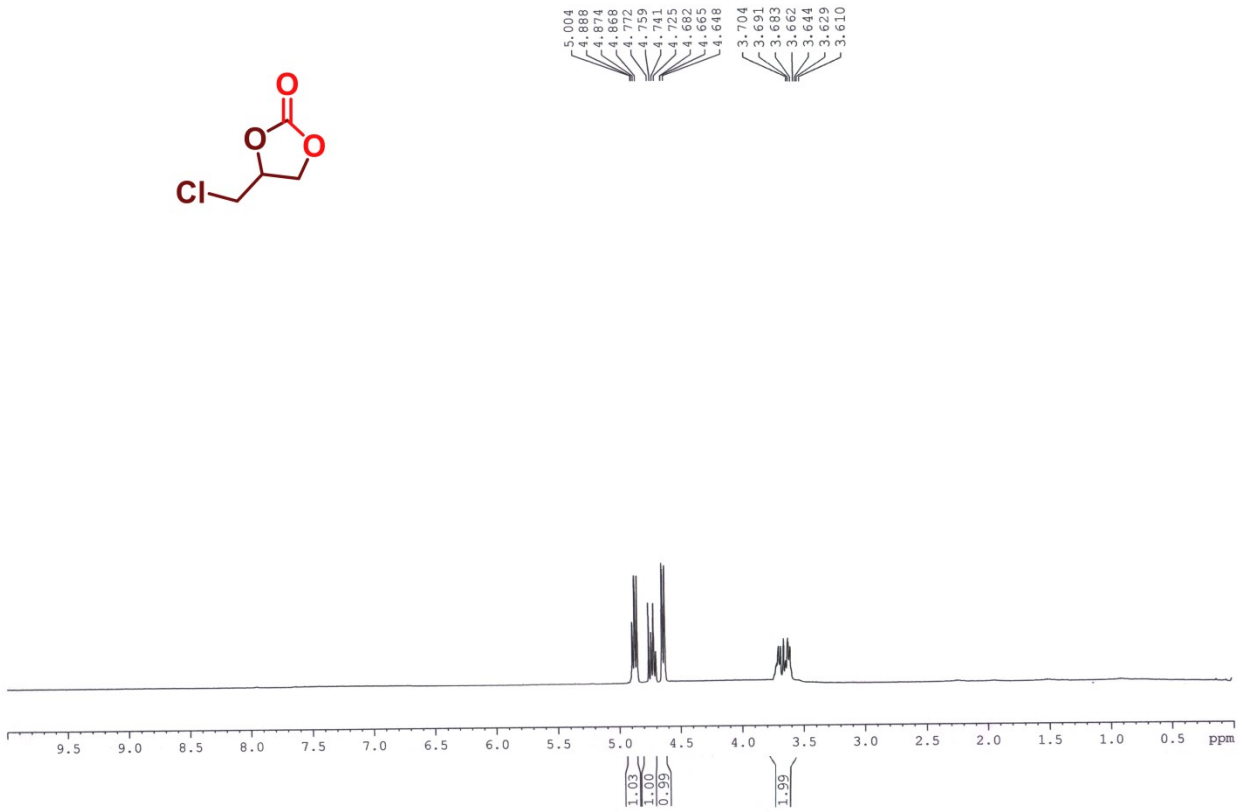

Figure S13: ^{1}H NMR spectra of 4-(chloromethyl)-1,3-dioxolan-2-one.

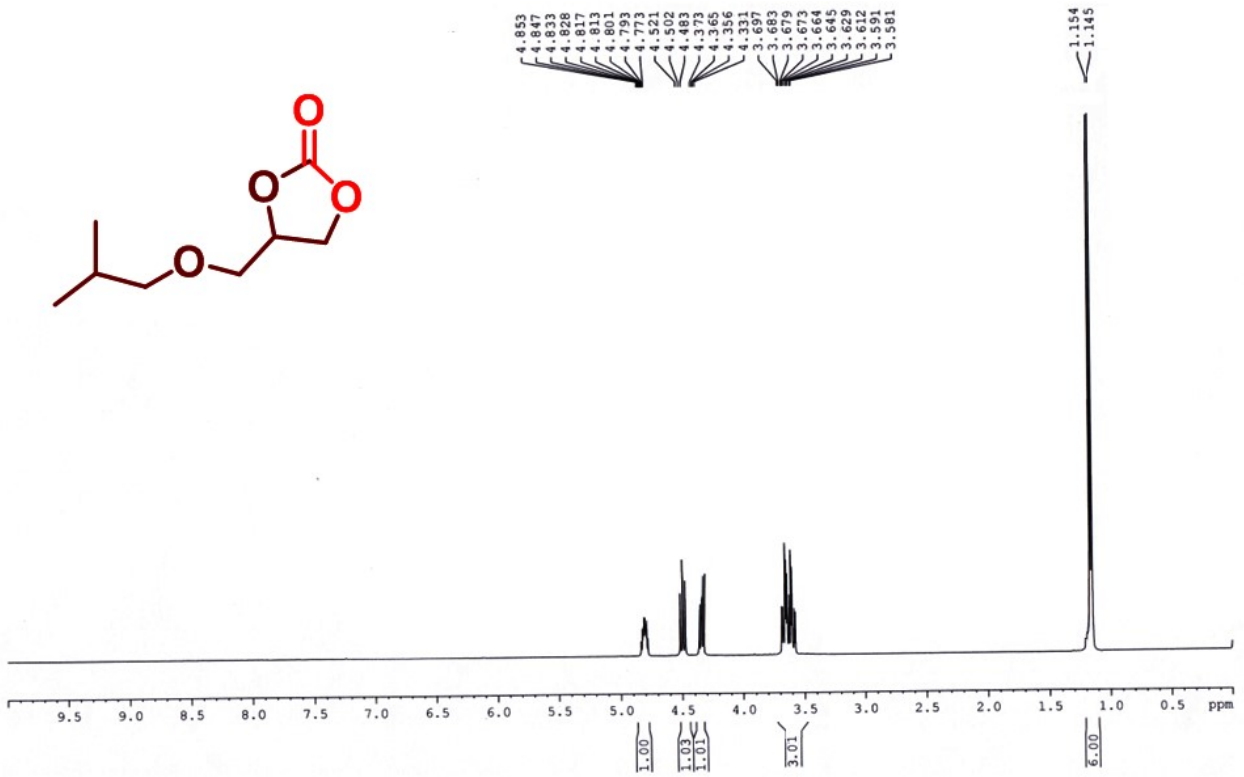

Figure S14: ^{1}H NMR spectra of 4-isobutoxy-1,3-dioxolan-2-one.

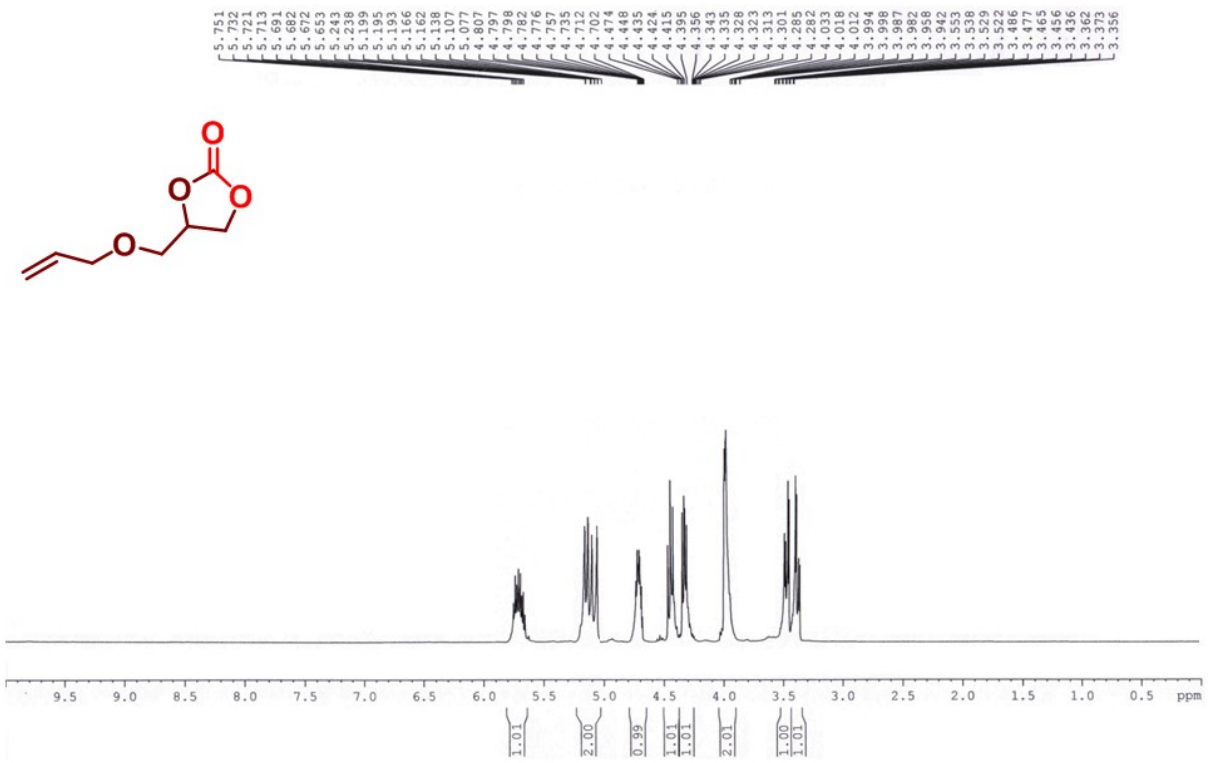

Figure 15: ^{1}H NMR spectra of 4-((allyloxy)methyl)-1,3-dioxolan-2-one.

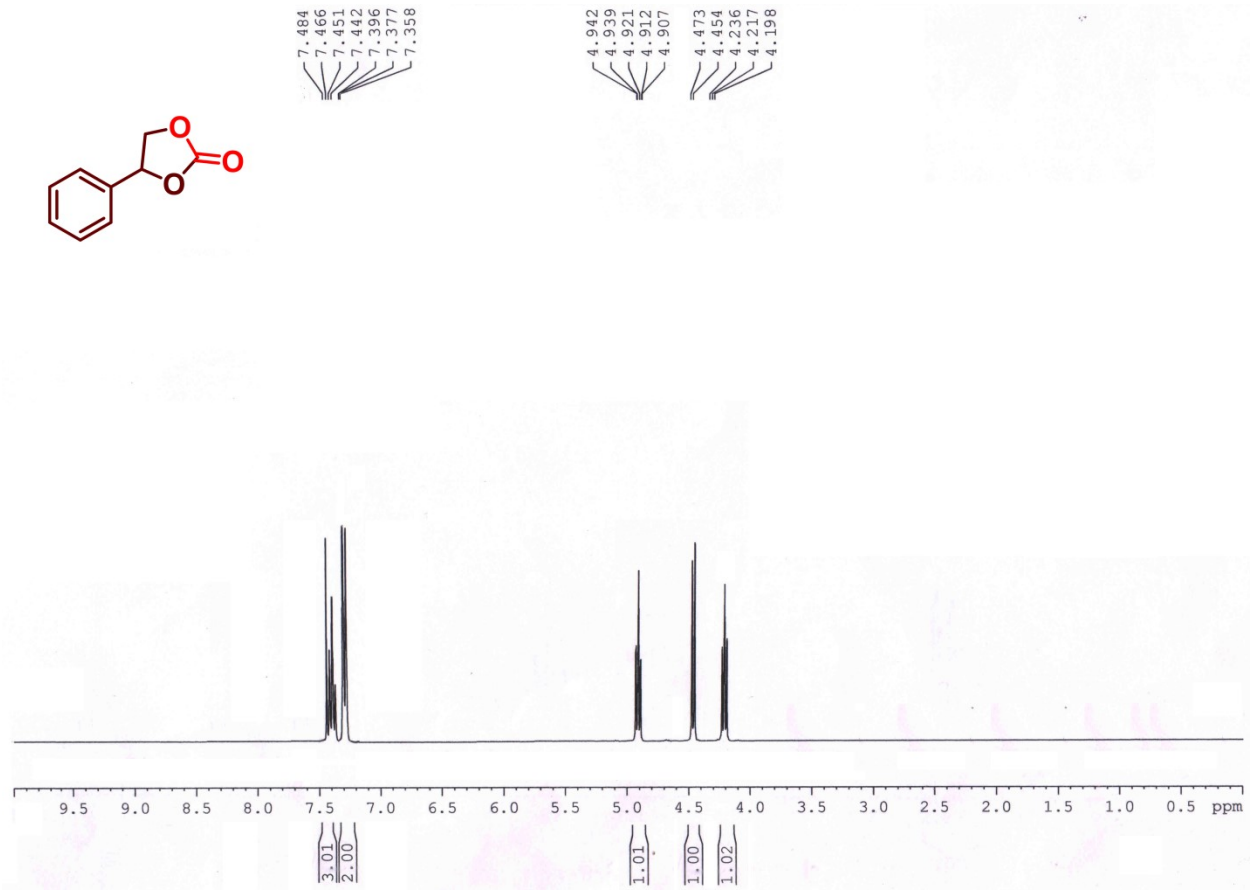

Figure S16: ^{1}H NMR spectra of 4-phenyl-1,3-dioxolan-2-one.

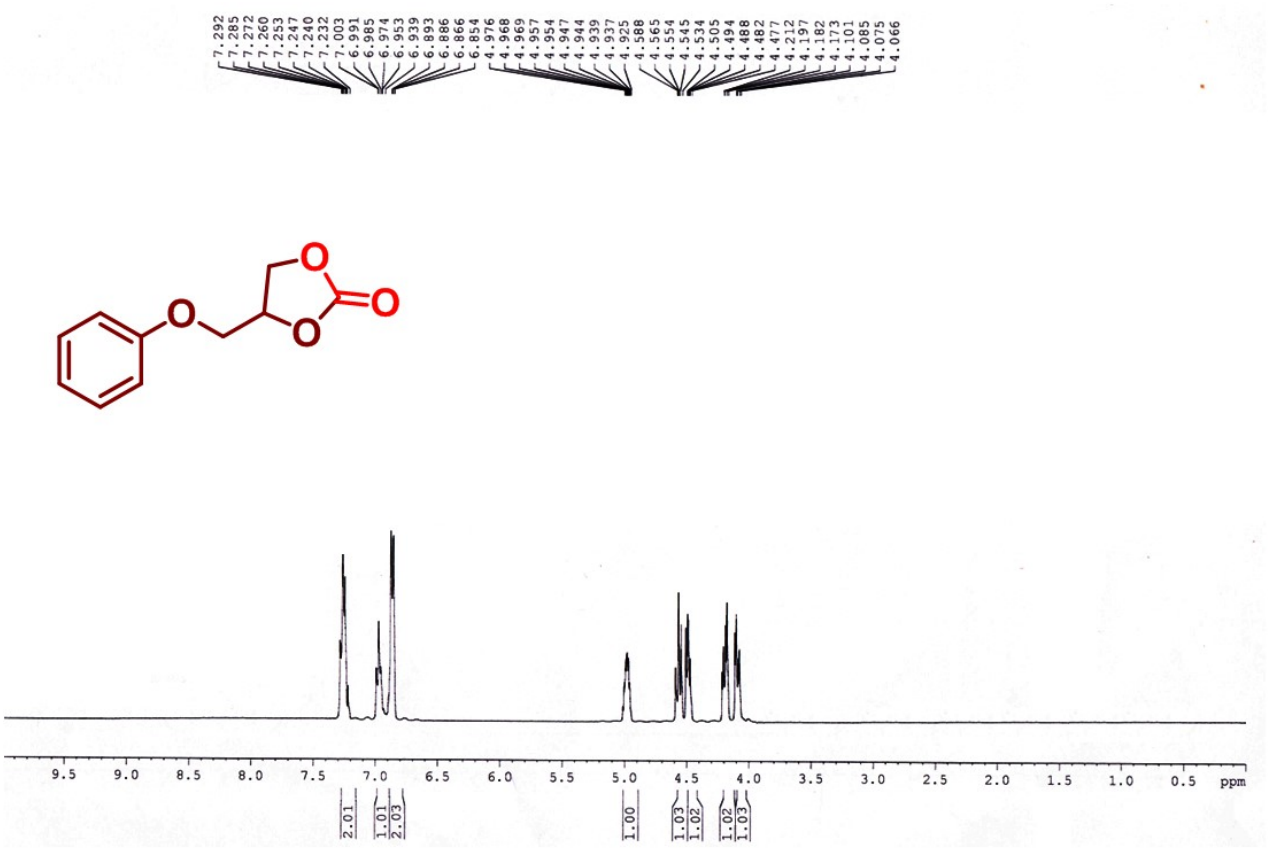

Figure S17: ^{1}H NMR spectra of 4-(phenoxymethyl)-1,3-dioxolan-2-one.

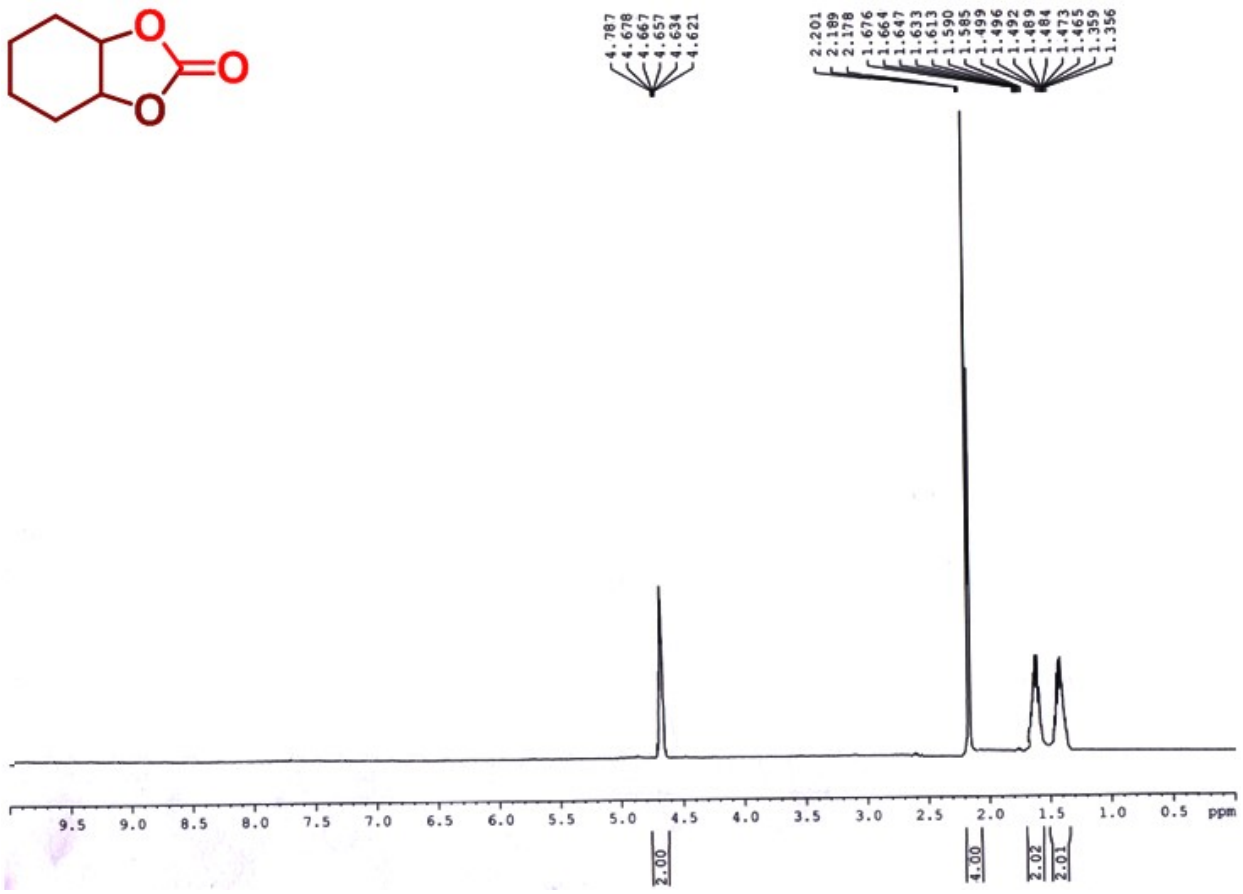

Figure S18**:** ^{1}H NMR spectra of hexahydrobenzo[d][1,3]dioxol-2-one.

References

(1) SMART (V 5.628), SAINT (V 6.45a),. *SMART (V 5.628), SAINT (V 6.45a), XPREP, SHELXTL, Bruker AXS Inc., Madison, WI,* **2004**. p 2004.

(2) Sheldrick, G. M. Crystal Paper Reference. *Acta Crystallographica Section C, Structural Chemistry*. **2015**, C71, 3–8.

(3) A. Altomare, M.C. Burla, M. Camalli, G. Cascarano, C. Giacovazzo, A. Guagliardi, A.G.G. Moliterni, G. Polidori and J. Spagna, *Appl. Cryst.* **1999**, 32, 115-119.

(4) van der Sluis, P. and Spek, A. L. *Acta Crystallographica Section A*, **1990**, A46, 194-201.

(5) Brandenburg, K. [or K. Brandenburg, & H. Putz, or K. Brandenburg, & M. Berndt,] *DIAMOND*. *Crystal Impact GbR,* 1999, *Bonn, Germany*.

(6) Parr, R. G. Density-Functional Theory of Atoms and Molecules. *Horizons Quantum Chem.* **1980**, 5–15.

(7) Becke, A. D. Density-Functional Thermochemistry. III. The Role of Exact Exchange. *J. Chem. Phys.* **1993**, *98*, 5648–5652.

(8) Lee, C.; Yang, W.; Parr, R. G. Development of the Colle-Salvetti Correlation-Energy Formula into a Functional of the Electron Density. *Phys. Rev. B* **1988**, *37*, 785–789.

(9) Frisch, M. J.; Trucks, G. W.; Schlegel, H. B.; Scuseria, G. E.; Robb, M. A.; Cheeseman, J. R.; Scalmani, G.; Barone, V.; Mennucci, B.; Petersson, G. A.; Nakatsuji, H.; Caricato, M.; Li, X.; Hratchian, H. P.; Izmaylov, A. F.; Bloino, J.; Zheng, G.; Sonnenberg, J. L.; Hada, M.; Ehara,M.; Toyota, K.; Fukuda, R.; Hasegawa, J.; Ishida, M.; Nakajima, T.; Honda, Y.; Kitao, O.; Nakai, H.; Vreven, T.; Montgomery J. A.Jr., Peralta, J. E.; Ogliaro, F.; Bearpark, M.; Heyd, J. J.; Brothers, E.; Kudin, K. N.; Staroverov, V. N.; Kobayashi, R.; Normand, J.; Raghavachari, K.; Rendell, A.; Burant, J. C.; Iyengar, S. S.; Tomasi, J.; Cossi, M.; Rega, N.; Millam, J. M.; Klene, M.; Knox, J. E.; Cross, J. B.; Bakken, V.; Adamo, C.; Jaramillo, J.; Gomperts, R.; Stratmann, R. E.; Yazyev, O.; Austin, A. J.; Cammi, R.; Pomelli, C.; Ochterski, J. W.; Martin, R. L.; Morokuma, K.; Zakrzewski, V. G.; Voth, G. A.; Salvador, P.; Dannenberg, J. J.; Dapprich, S., Daniels, A. D.; Farkas, Ö.; Foresman, J. B.; V Ortiz, J.; Cioslowski, J.; Fox, D. J.; *Gaussian Inc.* **2009**, Wallingford CT.

(10) S. Muthuramalingam, M. Velusamy and R. Mayilmurugan, *Dalton Trans.*, 2021, **50**, 7984–7994